J Appl Physiol 102: 1193–1201, 2007.
First published October 26, 2006; doi:10.1152/japplphysiol.00491.2006.

Sensitivity of the cross-correlaton between simulated surface EMGs for two muscles to detect motor unit synchronization

Kevin G. Keenan,[1] Dario Farina,[2] François G. Meyer,[3] Roberto Merletti,[4] and Roger M. Enoka[1]

[1]*Departments of Integrative Physiology, and* [3]*Electrical and Computer Engineering, University of Colorado at Boulder, Boulder, Colorado;* [2]*Department of Health Science and Technology, Center for Sensory-Motor Interaction (SMI), Aalborg University, Aalborg, Denmark; and* [4]*Dipartimento di Elettronica, Laboratorio di Ingegneria del Sistema Neuromuscolare (LISiN), Politecnico di Torino, Torino, Italy*

Submitted 29 April 2006; accepted in final form 24 October 2006

Keenan KG, Farina D, Meyer FG, Merletti R, Enoka RM. Sensitivity of the cross-correlaton between simulated surface EMGs for two muscles to detect motor unit synchronization. *J Appl Physiol* 102: 1193–1201, 2007. First published October 26, 2006; doi:10.1152/japplphysiol.00491.2006.—The purpose of the study was to evaluate the use of cross-correlation analysis between simulated surface electromyograms (EMGs) of two muscles to quantify motor unit synchronization. The volume conductor simulated a cylindrical limb with two muscles and bone, fat, and skin tissues. Models of two motor neuron pools were used to simulate 120 s of surface EMG that were detected over both muscles. Short-term synchrony was established using a phenomenological model that aligned the discharge times of selected motor units within and across muscles to simulate physiological levels of motor unit synchrony. The correlation between pairs of surface EMGs was estimated as the maximum of the normalized cross-correlation function. After imposing four levels of motor unit synchrony across muscles, five parameters were varied concurrently in the two muscles to examine their influence on the correlation between the surface EMGs: *1*) excitation level (5, 10, 15, and 50% of maximum); *2*) muscle size (350 and 500 motor units); *3*) fat thickness (1 and 4 mm); *4*) skin conductivity (0.1 and 1 S/m); and *5*) mean motor unit conduction velocity (2.5 and 4 m/s). Despite a constant and high level of motor unit synchronization among pairs of motor units across the two muscles, the cross-correlation index ranged from 0.08 to 0.56, with variation in the five parameters. For example, cross-correlation of EMGs from pairs of hand muscles, each having thin layers of subcutaneous fat and mean motor unit conduction velocities of 4 m/s, may be relatively insensitive to the level of synchronization across muscles. In contrast, cross-correlation of EMGs from pairs of leg muscles, with larger fat thickness, may exhibit a different sensitivity. These results indicate that cross correlation of the surface EMGs from two muscles provides a limited measure of the level of synchronization between motor units in the two muscles.

electromyograms; model; motor neuron; synchrony

BECAUSE COMMON SYNAPTIC INPUTS onto motor neuron pools can cause coincidental discharges of action potentials by motor neurons, the correlated discharge of motor units is often used as an index of the common synaptic input received by the motor neuron pool (10, 48, 53). The level of correlation can be quantified as motor unit synchronization by cross-correlating the discharge times of pairs of concurrently active motor units. Although most studies have focused on motor unit synchrony within muscles (18, 56), several studies have examined synchrony across muscles (7, 29, 52).

Due to the limitations associated with extrapolating from the data obtained on a few pairs of motor units to the population (54), indexes based on the cross-correlation of surface electromyograms (EMGs) have been used to represent population levels of motor unit synchrony across muscles (25, 26, 39). One method involves correlation in the time domain and is suggested to provide information on common inputs onto the motor neuron pools (21, 25, 31, 38). This cross-correlation technique assumes that the EMG signals contain information on the timing of the synchronized motor unit discharges. However, the two EMG signals can be influenced by variation in a number of physiological parameters that may confound this assumption (16). For example, the shapes of motor unit potentials of synchronized units in the two muscles, and hence their contribution to the interference EMGs, will vary due to differences in fiber length, the locations of the motor units relative to the recording electrodes, and the conduction velocities of the action potentials (16).

To identify the influence of these different factors, a computational approach was used. This strategy has proved useful for examining motor unit populations (19, 41, 52) and assessing the sensitivity of the surface EMG to selected parameters (4, 9, 15). The purpose of the study was to evaluate the use of cross-correlation analyses between simulated surface EMGs of two muscles to quantify motor unit synchronization. Short-term synchrony was imposed at varying levels within and across muscles by aligning motor unit discharge times, and the influence of selected physiological parameters on the time-domain measure of cross-correlation between surface EMGs was examined.

METHODS

The study involved computer simulations that were based on a model of recruitment of a population of motor units (20) with the addition of an EMG model (17) that simulated the surface EMG detected above two muscles within a cylindrical limb containing bone, muscle, fat, and skin tissues. The simulations comprised five main steps: *1*) determining the recruitment and discharge times of two populations of motor neurons in response to different levels of excitation; *2*) imposing physiological levels of synchrony within and across muscles; *3*) generating motor unit potentials from estimates of the number, location, and conduction velocities of the muscle fiber action potentials for each motor unit; *4*) simulating the surface EMG by summing the trains of motor unit potentials; and *5*) estimating the correlation between pairs of surface EMGs as the maximum of the

Address for reprint requests and other correspondence: R. M. Enoka, Dept. of Integrative Physiology, Univ. of Colorado, Boulder, CO 80309-0354 (e-mail: enoka@colorado.edu).

The costs of publication of this article were defrayed in part by the payment of page charges. The article must therefore be hereby marked "*advertisement*" in accordance with 18 U.S.C. Section 1734 solely to indicate this fact.

normalized cross-correlation function. The selected parameters that were varied concurrently in the two muscles to examine their influence on the cross-correlation function included excitation level, muscle size, fat thickness, skin conductivity, and mean motor unit conduction velocity.

Surface EMG Simulations

The model was implemented in Matlab version 6.5 (The Mathworks, Natick, MA). The basic parameters for the model of the two muscles in an idealized cylindrical limb are presented in Table 1. The distributions of properties across the motor unit pool were based on the Size Principle (28), and these included innervation number, recruitment threshold, motor unit territory, and conduction velocity of motor unit potentials.

Volume conductor. The cylindrical volume conductor (Fig. 1) consisted of a bone (20-mm radius) that was surrounded by an anisotropic muscle layer (50-mm radius), a fat layer (1 or 4 mm thick), and a skin layer (1 mm thick). Two muscles were simulated in the muscle layer: a large muscle that had 500 motor units and a small muscle that had 350 motor units. The cross sections of both muscles were simulated as ellipses with the axes of 30 and 60 mm for the large muscle and 22 and 30 mm for the small muscle. The number of muscle fibers was 260,017 and 95,339 for the large and small muscles, respectively (Table 1), based on a mean muscle fiber area of 5,437 μm^2 (43), a muscle cross-sectional area of 1,413 mm^2 and 518 mm^2, respectively, and an estimation that 20% of the cross-sectional area comprised noncontractile tissue (30). Three comparisons were made between muscles: *1*) two large muscles with centers located 90° apart (Fig. 1*A*); *2*) one small muscle and one large muscle with the centers

Table 1. *Table of model parameters*

Model Parameters	Values
Motor unit conduction velocity	
Mean	4† and 2.5* m/s
Standard deviation (Gaussian distribution)	0.4 m/s
Conductivities (S/m)	
Bone	0.02
Muscle (radial and transverse)	0.1
Muscle (longitudinal)	0.5
Subcutaneous tissue	0.05
Skin	1* and 0.1†
Large muscle	
Number of motor units	500
Muscle cross-sectional area	1413 mm^2
Number of fibers	260,017
Innervation number: average (range)	520 (24–2408)
Average fiber length	130 mm
Small muscle	
Number of motor units	350
Muscle cross-sectional area	518 mm^2
Number of fibers	95,339
Innervation number: average (range)	272 (14–1410)
Average fiber length	80 mm
Skin thickness	1 mm
Subcutaneous tissue thickness	1† and 4* mm
Innervation zone	
Width (standard deviation of uniform distribution)	5 mm
Horizontal location (% along fiber length)	50%
Tendon ending spread (uniform distribution)	5 mm
Electrodes	
Circular (diameter)	8 mm
Interelectrode distance	20 mm
Distance of detection system from center of innervation zone	
Large muscle	32.5 mm
Small muscle	20 mm
Separation of detection systems around cylinder	
Two large muscles	90† degrees
One small and one large muscle	67.5 degrees
Two small muscles	45* degrees
Excitation level (% maximum)	5*, 10, 15, and 50†%
Synchrony level (average CIS)	
Within muscle	0, 0.2, 0.4, 0.6, 0.8, and 1
Across muscles	0, 0.2, 0.4, and 0.6

CIS, common input strength. *Condition that resulted in the maximal cross-correlation index. †Condition that resulted in the minimal cross-correlation index.

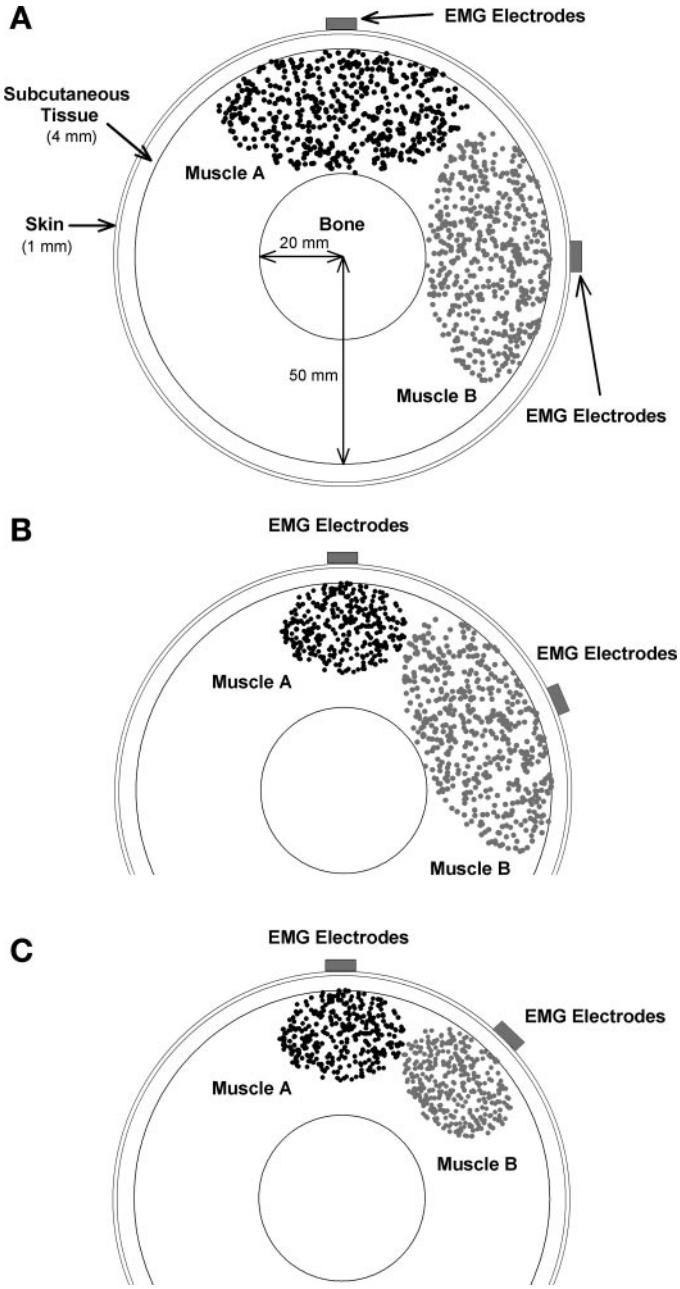

Fig. 1. Cross section of the simulated volume conductor. Points represent the random location of the center of the motor units for two large muscles with 500 motor units in each muscle (*A*); one small muscle with 350 motor units and one large muscle (*B*); and two small muscles (*C*). The radial position of the bipolar surface electromyogram (EMG) detection systems is shown above the center of each muscle.

located 67.5° apart (Fig. 1*B*); and *3*) two small muscles with centers located 45° apart (Fig. 1*C*).

Generation of muscle fiber potentials. Each tissue layer was homogeneous, and the conductivity properties of each layer (Table 1) were similar to those reported by Farina et al. (17). The muscle layer was anisotropic and more conductive in the longitudinal than the transverse fiber direction, whereas the bone, subcutaneous, and skin tissues were isotropic. Two values for skin conductivity were chosen since higher values may influence cross talk and the amplitude of the cross-correlation function (41).

Average fiber length was 130 and 80 mm for the large and small muscles, respectively, and the center of the innervation zones for both large and small muscles were located at 50% of the length of the fibers and in the same transverse location within the volume conductor. The end plate and insertion of each fiber into the tendons varied randomly (uniform distribution) over a range of 5 mm. The electrodes were simulated as circular (8-mm diameter) and arranged in bipolar pairs (20-mm interelectrode distance) along the direction of the muscle fibers. The electrodes were located halfway between the innervation zone and the distal tendon and were placed directly over the center of the muscle in the radial direction (Fig. 1). The simulation of the intracellular action potential was based on the analytical description of Rosenfalk (51). The surface-recorded, motor unit potential comprised the sum of the action potentials of the muscle fibers belonging to the motor unit. Motor unit potentials and the EMG signal were computed at 4,096 samples/s.

Motor unit properties. The distribution of the motor units within the muscle (32, 44) was determined by randomly selecting the *x-y* coordinates corresponding to the center of each motor unit territory within the elliptical cross section of the muscle. The fibers of a motor unit were randomly scattered in the motor unit territory (58) with a density of 20 fibers/mm^2 (2) and interdigitated with fibers belonging to many other units. The territories of the largest motor units, therefore, were greater than those of the smallest motor units (5). To restrict the distribution of the fibers of a motor unit (5, 58), motor unit territories were modeled to be circular (8). The radius of the motor unit territory was based on the density of fibers and the assigned innervation number of the motor unit. However, when a portion of the motor unit territory was constrained by the muscle boundary, the territory of the unit was modified to fit the muscle cross section, and fiber density was changed to accommodate the required number of motor unit fibers within the new territory. The result of constraining the motor unit territory had little influence on fiber density for small motor units but increased fiber density for the largest motor units, consistent with experimental findings (2, 33). In previous versions of the model (20, 63), motor unit territories were restricted to be circular and within the muscle; thus the largest motor unit territories overlapped within the center of the muscle, resulting in high fiber densities. In the current version of the model, constraining the motor unit territories resulted in a more uniform fiber density throughout the muscle.

To match the exponential relation between the number of motor units and motor unit force (35, 37, 45) and the high correlation between innervation number and tetanic force of a motor unit (6, 33), the number of fibers innervated by a single motor neuron increased exponentially from the smallest to the largest motor unit. Innervation numbers in the current study ranged from 24 to 2,408 for the large muscle and from 14 to 1,410 fibers for the small muscle based on an ~100-fold range of twitch forces (13, 45, 60). The motor units had mean muscle fiber conduction velocities of either 4 ± 0.4 or 2.5 ± 0.4 m/s (14), with the smallest motor units assigned the slowest conduction velocities (1).

Activation characteristics. Activation of the motor unit pool was modeled as a ramp-and-hold function, with a 1-s ramp increase in excitation to a mean level that was constant for 119 s. The distribution of recruitment thresholds for the motor neurons was represented as an exponential function with many low-threshold neurons and progressively fewer high-threshold neurons (11, 46). Each motor unit began discharging at 8 pulses/s (pps) once excitation exceeded the assigned recruitment threshold of the unit, and discharge rates increased linearly with increases in excitation. Excitation refers to the simulated net synaptic input onto the motor neuron pool (27), and it was assumed that all neurons received the same level of excitation. Although excitation level was similar, the response of the neurons differed based on their assigned recruitment thresholds, thereby allowing simulated input-output functions of the motor neurons to be specified by observed relations between discharge rate and injected current (36).

Maximal excitation was denoted as the level of input necessary to bring the last recruited motor neuron to its assigned peak discharge rate and values of excitation were expressed as a percentage of the maximal input. To match experimental reports (23, 46), peak discharge rates increased linearly with recruitment threshold in the range of 25–35 pps. The last unit was recruited at 79% maximal excitation for both muscles sizes, matching the range observed in many limb muscles (3, 11). Variability in discharge rate was modeled as a random process with a Gaussian distribution and a coefficient of variation set at 20%. Motor unit activity and associated surface EMG signals were simulated for the two muscles when both muscles were active at 5, 10, 15, and 50% of maximal excitation.

Motor unit synchronizaton. Motor unit synchronization was simulated by using a phenomenological model (47, 59, 63) that adjusted the timing of selected action potentials to impose a temporal association between action potentials discharged by different motor neurons. The scheme imposed motor unit synchrony first within *muscle A* and then by aligning discharge times of units in *muscle B* with units in *muscle A*. Motor unit synchronization was quantified with the common input strength (CIS) index as the number of synchronous counts above chance in the cross-correlation histogram constructed from the discharge times of pairs of motor units relative to the duration of the trial (extra counts/s; Ref. 48). CIS values were calculated and averaged for 50 randomly selected pairs of motor units either within or across muscles to quantify synchronization.

Within-muscle synchrony. Motor unit synchrony was imposed within *muscle A* at six levels by applying a function that selected between 0, 1.4, 3.4, 5.0, 7.4, and 10.1% of the action potentials discharged by each motor unit to be synchronized with eight other motor units. Discharge times of the reference motor unit were selected randomly, and when a discharge time of another randomly selected motor unit occurred within ±30 ms of the discharge by the reference motor unit, this discharge time was aligned with the reference unit with a Gaussian distribution that had a standard deviation of 1.67 ms centered on the reference unit. This process was repeated until the discharge times of eight other motor units were aligned with the discharge time of the reference motor unit for each discharge of the reference motor unit selected for this adjustment and ad seriatim for all motor units in the pool. The six levels of motor unit synchronization were chosen to generate average CIS values within *muscle A* (CIS_{wm}) of 0.0, 0.2, 0.4, 0.6, 0.8, and 1.0 (Table 1), which match the range of values observed experimentally within many muscles (29, 55).

Previous studies have demonstrated that selecting a proportion of the discharges to be synchronized with a proportion of the other motor units resulted in varying CIS levels across the active motor units (59, 63). Specifically, motor unit pairs with the highest recruitment thresholds active at a given excitation level had lower CIS values than the mean value calculated across all pairs. To impose a uniform CIS level across the entire motor unit pool, the current scheme imposed synchrony across a set number of motor units (47).

Across-muscle synchrony. To evaluate the influence of motor unit synchrony among motor units in two muscles, four levels of synchrony across the two muscles were simulated. For this condition, the discharge times of motor units in *muscle A* were randomly selected, to which the discharge times of motor units in *muscle B* were aligned

according to the procedure described above. To impose synchrony across muscles, the discharge times of the units in *muscle B* were moved to coincide with those in *muscle A*. Four levels of motor unit synchronization were chosen to generate average CIS values across muscles (CIS_{am}) of 0.0, 0.2, 0.4, and 0.6 (Table 1). These values matched the range observed experimentally across muscles (29, 34, 61). The percentage of discharge times from each unit that were moved to achieve the requisite level of synchrony across muscles was 0, 4.1, 9.8, and 16.7% for CIS_{am} levels of 0.0, 0.2, 0.4, and 0.6, respectively.

Analysis of Simulated Surface EMGs

Selected conditions (Table 1) were varied concurrently in both muscles to determine their influence on the correlation between pairs of surface EMGs. Because the distribution of motor unit locations alters the surface EMG signal and may influence the level of correlation between pairs of surface EMGs, the measurements were calculated from 20 simulations with randomly varying location of the motor units in each muscle for each simulation. Variability in the time-domain measure of correlation across the 20 random motor unit locations for the simulated conditions was small (<5%), however, so only means are reported in the text and figures.

The cross-correlation function (R_{xy}) was calculated from pairs of interference EMGs recorded over the concurrently activated muscles and normalized with respect to the square root of the product of the autocorrelation of both signals at zero time lag (62). The maximal R_{xy} will be referred to as the cross-correlation index. To examine the influence of cross talk on the cross-correlation index, the EMG contributed by activation of the muscle not directly under the recording electrodes was removed before the two signals were correlated. Specifically, the EMG contributed by *muscle B* to the electrodes over *muscle A* (Fig. 1) and the contribution of *muscle A* to the electrodes over *muscle B* were subtracted from the EMGs that resulted from concurrent activation of both muscles.

RESULTS

Selected parameters were adjusted to examine their influence on the cross-correlation index. These parameters included excitation level, motor unit conduction velocity, muscle size, fat thickness, and skin conductivity.

Influence of Motor Unit Synchrony

The influence of motor unit synchronization on the cross-correlation index varied across the simulated conditions. Representative data are shown for the condition (asterisks in Table 1) that resulted in the maximal cross-correlation index between surface EMG recordings after imposing motor unit synchrony across muscles (Fig. 2). Synchronization between randomly selected pairs of motor units was first imposed within *muscle A* ($CIS_{wm} = 0.6$), and then selected discharge times in *muscle B*

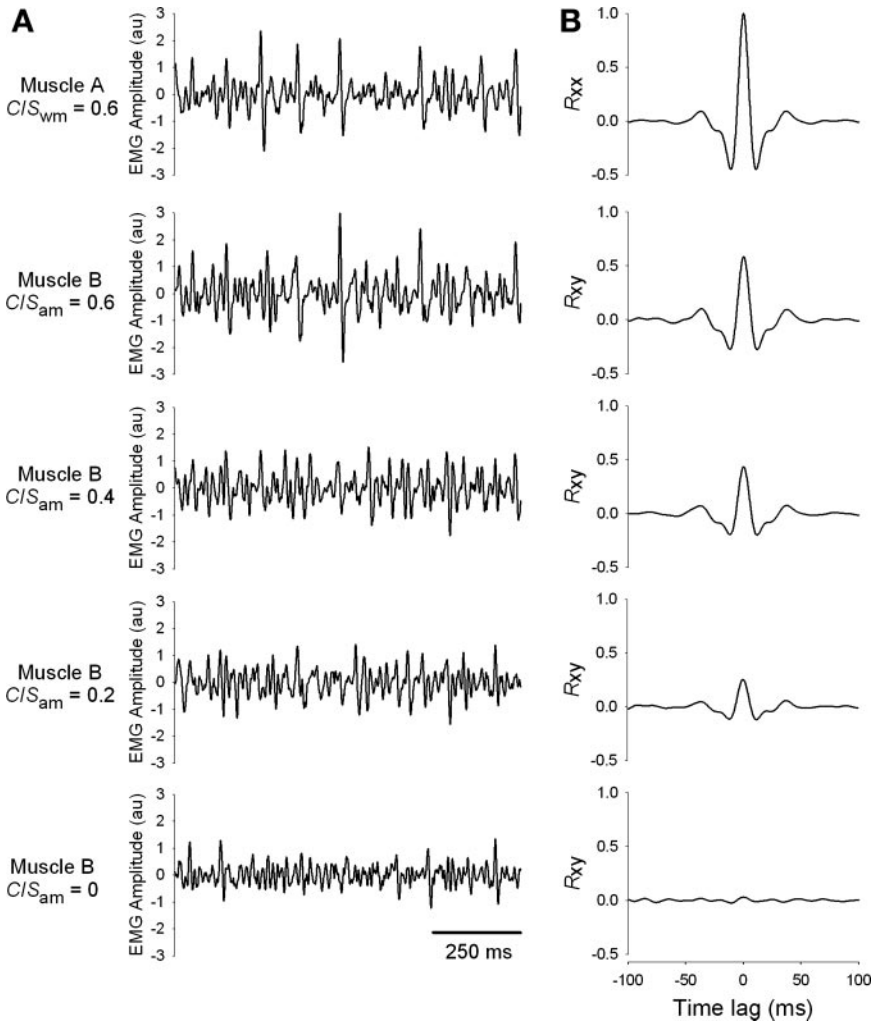

Fig. 2. Representative data for the condition that resulted in the maximal cross-correlation index (Table 1) between surface EMG recordings after imposing motor unit synchrony across muscles. *A*: *top* trace shows the EMG signal detected over *muscle A* with an average common input strength (CIS) of 0.6 within the muscle (CIS_{wm}). *Traces 2–5* depict the surface EMG over *muscle B* after varying levels of synchrony were imposed across the two muscles (CIS_{am}), which involved the alignment of motor unit discharge times in *muscle B* to those in *muscle A*. *B*: *top* trace indicates the autocorrelation for the EMG signal for *muscle A* (*trace 1*, *panel A*), and *traces 2–5* denote the cross-correlation function between the EMGs recorded over the two muscles. The cross-correlation index increased up to ~0.6, with increases in motor unit synchronization across muscles for this condition (marked by asterisks in Table 1). au, Arbitrary units; *R*xy, cross-correlation function.

were aligned with the discharge times in *muscle A* (CIS_{am} = 0.6–0.0; 4 levels). Interference EMGs detected above *muscle A* (Fig. 2, *top*) and above *muscle B*, with varying levels of across-muscle synchronization between motor units, are shown in Fig. 2*A*. Representative cross-correlations are shown in Fig. 2*B* between the EMGs for the two muscles; the top trace indicates the autocorrelation function for the *muscle A* signal. For this condition (asterisks in Table 1), the cross-correlation index increased up to ~0.6 with an increase in motor unit synchronization from CIS_{am} = 0–0.6.

Influence of Cross Talk

The increase in the cross-correlation index due to motor unit synchronization was not influenced by cross talk. In addition to the conventional cross-correlation index (solid lines in Fig. 3*A*), the cross-correlation analysis was performed after removing the EMG signal contributed by each muscle to the recording over the other muscle. Cross correlations for the condition without cross talk (dotted lines in Fig. 3*A*) are shown for four levels of across-muscle synchrony. There was little change in the cross-correlation index after removal of cross talk, even when the cross-correlation index was maximized (asterisks in Table 1) by the closest spacing between muscles and electrodes, the thicker subcutaneous tissue, and a higher skin conductivity, which are conditions that are expected to increase cross talk (41, 50, 57).

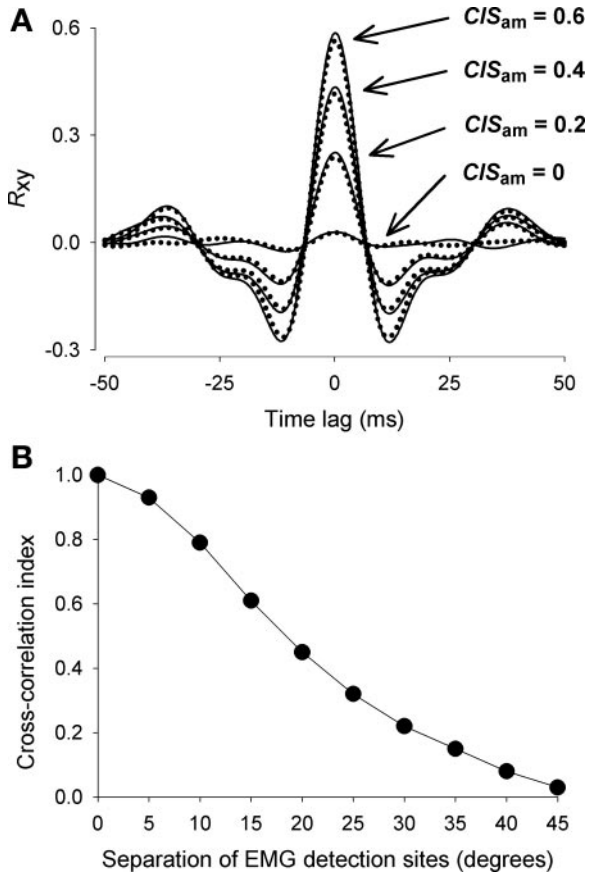

Fig. 3. Influence of cross talk on the cross-correlation index. *A*: the cross-correlations from Fig. 2 are depicted for the 4 levels of CIS_{am} (0, 0.2, 0.4, and 0.6), with (solid line) and without (dotted line) cross talk. The cross-correlation index was minimally influenced by the removal of cross talk, which indicates that cross-correlation between EMG signals from nearby muscles does not reflect cross talk between the muscles. *B*: the influence of cross talk on the cross-correlation index was then examined by varying the distance between EMG detection systems. Cross correlations were computed for the set of parameters that resulted in the maximal cross-correlation index (Table 1) and that would be expected to increase the magnitude of cross talk (41, 50, 57). EMG detection systems were positioned between the two muscles and were separated by 0–45° (5° increments) along the radial location of the volume conductor (Fig. 1*C*). The cross-correlation index decreased with increasing distance between the EMG detection systems.

To confirm that cross talk could influence the cross-correlation function, the cross-correlation analysis was performed on EMGs detected without motor unit synchronization across muscles and after varying the separation between the two EMG detection systems (Fig. 3*B*). Data are shown for the condition (asterisks in Table 1) that resulted in the maximal cross-correlation index between surface EMG recordings and that would be expected to maximize the influence of cross talk. EMG detection systems were modeled first to be at the identical radial location between the two muscles (0° separation) and then progressively separated by 5° intervals up to 45°. The cross-correlation index decreased with increasing distance between detection systems, reaching a minimum at ~45°, consistent with a study that examined the influence of cross talk on the cross-correlation index in more detail (41).

Factors that Influenced the Cross-Correlation Index

To quantify the influence of different parameters on the cross-correlation index, four levels of motor unit synchronization were imposed across muscles (CIS_{am} = 0–0.6; Fig. 4, *x*-axis) and the cross-correlation index was generated for concurrent adjustments in all other parameters (Table 1). The result was a total of 96 conditions at each level of motor unit synchronization, and the effect on the cross-correlation index is shown in Fig. 4. There was a set of conditions that maximized the influence of motor unit synchronization on the cross-correlation index (R_{xy}) between the surface EMG recordings and another set that minimized R_{xy} (Table 1). For the condition that maximized R_{xy}, the cross-correlation index increased up to ~0.6, with an increase in motor unit synchronization across muscles (Fig. 4). In contrast, the condition that minimized R_{xy} caused the cross-correlation index to increase less, up to 0.08 (Fig. 4), although the level of across-muscle synchronization was high (CIS_{am} = 0.6).

Further analysis examined why variation in parameters that influenced only the individual motor unit potentials, such as mean motor unit conduction velocity, skin conductivity, and subcutaneous tissue thickness, had such a large effect on the cross-correlation index. Figure 5 shows the three largest amplitude potentials for the motor units that were active at 5% maximal excitation in the small muscle when generated with the parameters (Table 1) that produced the maximal (Fig. 5*A*) and minimal (Fig. 5*B*) cross-correlation indexes. For these two conditions, the same motor unit potentials were used for both *muscles A* and *B* to demonstrate the influence of shape on the cross-correlation index. Random variability in the timing of the potentials shown in Fig. 5 has been added (SD = 1.67 ms; Gaussian distribution) for both *muscles A* and *B*, which is identical to the variability added when imposing motor unit synchronization. The variability in timing was the same for motor units in Fig. 5, *A* and *B*. Due to variation in the shapes

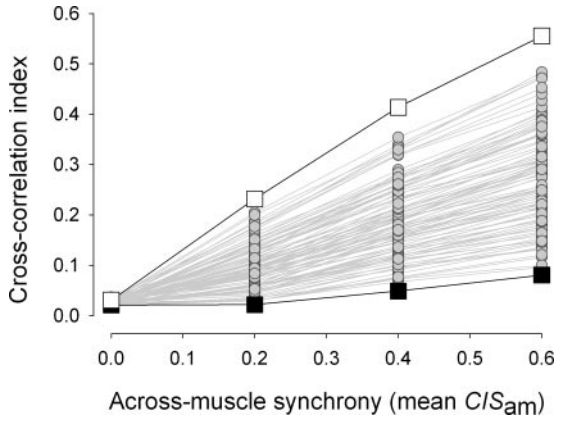

Fig. 4. The increase in the cross-correlation index with increased CIS_{am} was sensitive to variation in all model parameters. Four levels of motor unit synchronization were imposed across muscles, and the cross-correlation index was generated for concurrent adjustments in all other parameters (Table 1), resulting in a total of 96 conditions at each level of motor unit synchronization. To demonstrate the range of all possible values, the cross-correlation index is shown for the conditions that resulted in the maximal (□) and minimal (■) cross-correlation index in the current study (Table 1). An increase in the level of CIS_{am} (0–0.6) resulted in a greater increase in the cross-correlation index between the pairs of surface EMGs when the condition involved a decrease in excitation level, muscle size, and motor unit conduction velocity, and an increase in fat thickness and skin conductivity (□).

of the motor unit potentials, however, the summed potentials were more variable for the condition in Fig. 5*B*. For the same variability in the timing of the potentials, the cross-correlation between summed motor unit potentials was greater for the maximal condition (0.99) compared with the minimal condition (0.68).

Table 2 summarizes the influence of each parameter on the cross-correlation index with varying levels of motor unit synchronization across the two muscles. For each simulation, the CIS level within *muscle A* was set at 0.6 and motor unit synchronization across muscles (CIS_{am}) varied from 0.0 to 0.6. Values for $CIS_{am} = 0$ are not shown since the cross-correlation index never exceeded 0.03. The cross-correlation index increased with an increase in motor unit synchronization for each of the simulated conditions, but variation in the value for each parameter led to variation in the magnitude of the correlation.

DISCUSSION

Although the cross-correlation index increased with the level of motor unit synchrony across muscles, variation in all of the parameters examined in the current study influenced the magnitude of the correlation. These parameters included excitation level, motor unit conduction velocity, muscle size, fat thickness, and skin conductivity. The results indicate that the cross-correlation analysis of surface EMGs from two muscles provides a limited estimate of the level of motor unit synchronization between the muscles.

Cross-Correlation Index

A recent simulation study found that the amplitude of the cross-correlation index was influenced by motor unit synchrony (41). They reported a high cross-correlation index ($R_{xy} = \sim 0.9$) during a simulated high-synchrony condition, which involved synchronizing 10% of the discharge times of all active motor units with 10% of other motor units within and across two simulated muscles. It was suggested, however, that the strong cross-correlation may have resulted from higher than physiological levels of motor unit synchronization. The current study indicates that, although motor unit synchrony does influence the cross-correlation index, so do many other parameters (Figs. 4 and 5; Table 2). The lower cross-correlation indexes in the present study compared with Lowery et al. (41) are attributable to such effects as shorter fiber lengths, greater variability in the alignment of the potentials of synchronized units, thinner layer of subcutaneous tissue, and a greater range in motor unit conduction velocities and innervation numbers. These findings suggest caution in interpreting changes in the cross-correlation index as indicative of variation in the level of motor unit synchronization.

The current study has practical implications for techniques that use cross-correlation in the time domain to detect motor unit synchrony. First, the magnitude of the change in the cross-correlation index needs to be considered in relation to the many factors that may influence the index. Although relatively small increases in the cross-correlation function between pairs of EMG signals have been used to suggest an increase in the amount of common input onto different motor neuron pools, this interpretation seems problematic because changes in other muscle parameters may cause the same result. Kilner et al. (38),

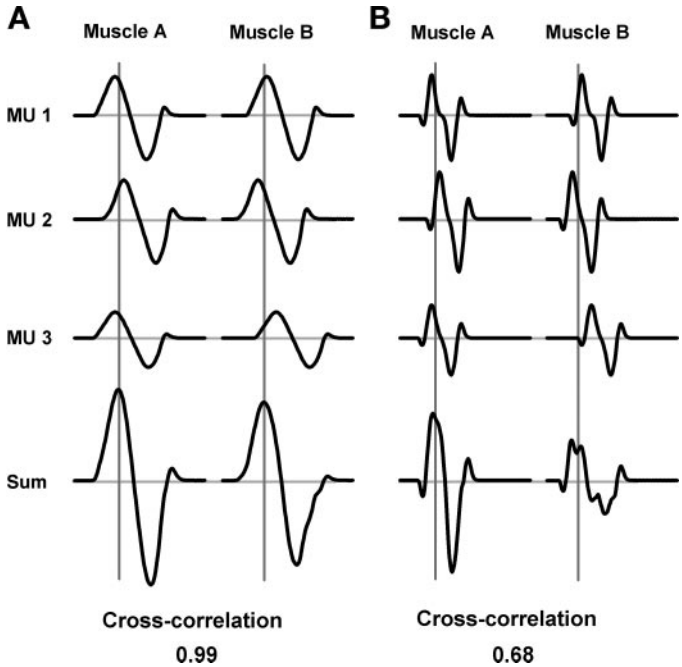

Fig. 5. Influence of the shape of the motor unit potentials on the cross-correlation index. An assumption of the cross-correlation technique is that the EMG signals contain information on the timing of the synchronized motor unit discharges and that the constituent potentials have similar shapes, thereby resulting in a high correlation between the two signals. The three largest potentials for motor units active at 5% maximal excitation in the small muscle are shown as generated for the conditions that resulted in the maximal (*A*) and minimal (*B*) cross-correlation index. For representative purposes, the same three potentials were summed for *muscles A* and *B* after imposing a random variability (SD = 1.67) between the activation times of the 3 units. The resulting cross-correlation index between the summed signals was 0.99 for the maximal condition (*A*) and 0.68 for the minimal condition (*B*). The difference in the amplitude of the cross-correlation function was attributable to variation in shapes of the summed potentials. MU, motor unit.

Table 2. *Mean (range) of the cross-correlation index across the 5 selected parameters in Table 1 after varying 1 parameter at a time in each muscle concurrently*

	*CIS_{am} = 0.6 Cross-Correlation Index	CIS_{am} = 0.4 Cross-Correlation Index	CIS_{am} = 0.2 Cross-Correlation Index
Excitation level			
5%	0.32 (0.11–0.56)	0.24 (0.11–0.41)	0.13 (0.05–0.23)
50%	0.21 (0.08–0.38)	0.16 (0.05–0.29)	0.06 (0.02–0.11)
Muscle size			
Small	0.33 (0.13–0.56)	0.22 (0.10–0.41)	0.12 (0.04–0.23)
Large	0.22 (0.08–0.41)	0.16 (0.05–0.33)	0.07 (0.02–0.17)
Skin conductivity, S/m			
1.0	0.33 (0.16–0.56)	0.24 (0.10–0.41)	0.12 (0.04–0.23)
0.1	0.21 (0.08–0.45)	0.15 (0.05–0.31)	0.08 (0.02–0.17)
Subcutaneous tissue, mm			
4	0.32 (0.14–0.56)	0.23 (0.09–0.41)	0.12 (0.03–0.23)
1	0.22 (0.08–0.46)	0.16 (0.05–0.32)	0.08 (0.02–0.18)
Mean conduction velocity, m/s			
2.5	0.30 (0.13–0.56)	0.22 (0.08–0.41)	0.11 (0.03–0.11)
4	0.24 (0.08–0.48)	0.17 (0.05–0.34)	0.08 (0.02–0.19)
Mean of above conditions	0.27 (0.08–0.56)	0.19 (0.05–0.41)	0.10 (0.02–0.23)

Values are means, with range in parentheses. *CIS_{am}, level of motor unit synchrony across muscles.

for example, suggested that differences in the cross-correlation function of ~0.1 between EMGs recorded over pairs of hand and wrist muscles during a precision grip task indicated task-dependent modulation of motor unit synchronization. Although Table 2 indicates that an increase in the cross-correlation index of ~0.1 could be due to an increase in motor unit synchronization, variation in any one parameter when an average CIS of 0.6 was imposed across muscles could change the cross-correlation index by this magnitude. Because experimental interventions can change many parameters that have varying effects on the cross-correlation index, the sensitivity to any one factor (e.g., motor unit synchrony) is obscured by the effect of the other parameters. These considerations are important when identifying changes in the cross-correlation function during walking (25), development (21), sustained submaximal contractions (49), between muscles in the upper and lower extremities (22), and when identifying muscle synergies (42).

Second, different techniques have been proposed to remove the confounding effect of cross talk before cross-correlation analysis is performed. For example, Kilner et al. (38) reported a process of double differentiation and a blind source-separation algorithm to remove cross talk before cross-correlating pairs of surface EMGs. However, mathematical differentiation of the EMG signal does not reduce cross talk (12). Furthermore, it is likely that cross talk has little effect on the cross-correlation index when electrodes are placed at a distance from one another, as reported by Lowery et al. (41) and demonstrated in Fig. 3. Consequently, it is probably not necessary to use advanced methods to remove cross talk before cross-correlation analysis.

Limitations

The current study used a phenomenological model to impose motor unit synchrony to replicate experimentally observed index CIS values in the simulated conditions. Although the current modeling approach was limited to selecting a proportion of the discharges of eight other motor units to impose a constant level of synchrony across the entire motor unit population, other phenomenological approaches (59, 63) produced similar results. In addition, although index CIS was the focus of the current study, CIS_{am} levels of 0.2, 0.4, and 0.6 at 5% maximal excitation resulted in average index E values of 0.02, 0.04, and 0.05, respectively, and k′ values of 1.21, 1.35, and 1.49, respectively. Although index E and k′ decreased systematically with an increase in excitation level, possibly due to the rate dependence of synchronization indexes (24), there was still variability in the cross-correlation index with increasing levels of synchronization across muscles for the conditions simulated in the study. Also, the phenomenological approach used to impose synchrony complicates separating the influence of within-muscle synchrony on across-muscle synchrony. For example, with a high level of synchrony within *muscle A*, the proportion of discharges in *muscle B* that were adjusted to establish a high level of synchrony across muscles is less than when synchrony is not imposed first within *muscle A*.

Simulations reported in this work were restricted to concurrent variations in specific muscle properties so that it was possible to examine their effect on cross-correlation analysis between pairs of surface EMGs in the time domain. An idealized volume conductor was simulated, and it is certain that variation in many different anatomical and motor unit properties could also influence the magnitude of the cross-correlation index. Also, the magnitude of the change in EMG amplitude with motor unit synchronization is influenced by the location of the recording electrodes relative to the underlying muscle fibers (40) and may pose practical limitations to the implementation of cross-correlation analyses.

In summary, although the level of motor unit synchronization across two muscles influenced the measure of cross-correlation between pairs of surface EMG signals, variation in many parameters had a large influence on the magnitude of the cross-correlation index. These results indicate limitations in techniques used to estimate population levels of motor unit synchronization from pairs of surface EMGs.

ACKNOWLEDGMENTS

The authors thank Dr. Nicolas Petersen for comments on a draft of this manuscript.

GRANTS

Research supported by awards from National Institutes of Health Grants NS-42734 and AG-09000 to R. M. Enoka.

REFERENCES

1. **Andreassen S, Arendt-Nielsen L.** Muscle fibre conduction velocity in motor units of the human anterior tibial muscle: a new size principle parameter. *J Physiol* 391: 561–571, 1987.
2. **Armstrong JB, Rose PK, Vanner S, Bakker GJ, Richmond FJ.** Compartmentalization of motor units in the cat neck muscle, biventer cervicis. *J Neurophysiol* 60: 30–45, 1988.
3. **Bigland-Ritchie B.** EMG/force relations and fatigue of human voluntary contractions. *Exerc Sport Sci Rev* 9: 75–117, 1981.
4. **Blok JH, Stegeman DF, van Oosterom A.** Three-layer volume conductor model and software package for applications in surface electromyography. *Ann Biomed Eng* 30: 566–577, 2002.
5. **Bodine SC, Garfinkel A, Roy RR, Edgerton VR.** Spatial distribution of motor unit fibers in the cat soleus and tibialis anterior muscles: local interactions. *J Neurosci* 8: 2142–2152, 1988.
6. **Bodine SC, Roy RR, Eldred E, Edgerton VR.** Maximal force as a function of anatomical features of motor units in the cat tibialis anterior. *J Neurophysiol* 57: 1730–1745, 1987.
7. **Bremner FD, Baker JR, Stephens JA.** Correlation between the discharges of motor units recorded from the same and from different finger muscles in man. *J Physiol* 432: 355–380, 1991.
8. **Buchthal F, Erminio F, Rosenfalck P.** Motor unit territory in different human muscles. *Acta Physiol Scand* 45: 72–87, 1959.
9. **Christakos CN.** A study of the electromyogram using a population stochastic model of skeletal muscle. *Biol Cybern* 45: 5–12, 1982.
10. **Datta AK, Stephens JA.** Synchronization of motor unit activity during voluntary contraction in man. *J Physiol* 422: 397–419, 1990.
11. **De Luca CJ, LeFever RS, McCue MP, Xenakis AP.** Behaviour of human motor units in different muscles during linearly varying contractions. *J Physiol* 329: 113–128, 1982.
12. **Dimitrova NA, Dimitrov GV, Nikitin OA.** Neither high-pass filtering nor mathematical differentiation of the EMG signals can considerably reduce cross-talk. *J Electromyogr Kinesiol* 12: 235–246, 2002.
13. **Elek JM, Kossev A, Dengler R, Schubert M, Wohlfahrt K, Wolf W.** Parameters of human motor unit twitches obtained by intramuscular microstimulation. *Neuromuscul Disord* 2: 261–267, 1992.
14. **Farina D, Fortunato E, Merletti R.** Noninvasive estimation of motor unit conduction velocity distribution using linear electrode arrays. *IEEE Trans Biomed Eng* 47: 380–388, 2000.
15. **Farina D, Merletti R.** A novel approach for precise simulation of the EMG signal detected by surface electrodes. *IEEE Trans Biomed Eng* 48: 637–646, 2001.
16. **Farina D, Merletti R, Enoka RM.** The extraction of neural strategies from the surface EMG. *J Appl Physiol* 96: 1486–1495, 2004.
17. **Farina D, Mesin L, Martina S, Merletti R.** A surface EMG generation model with multilayer cylindrical description of the volume conductor. *IEEE Trans Biomed Eng* 51: 415–426, 2004.
18. **Farmer SF, Bremner FD, Halliday DM, Rosenberg JR, Stephens JA.** The frequency content of common synaptic inputs to motor neurones studied during voluntary isometric contraction in man. *J Physiol* 470: 127–155, 1993.
19. **Fortier PA.** Use of spike triggered averaging of muscle activity to quantify inputs to motor neuron pools. *J Neurophysiol* 72: 248–265, 1994.
20. **Fuglevand AJ, Winter DA, Patla AE.** Models of recruitment and rate coding organization in motor-unit pools. *J Neurophysiol* 70: 2470–2488, 1993.
21. **Gibbs J, Harrison LM, Stephens JA.** Cross-correlation analysis of motor unit activity recorded from two separate thumb muscles during development in man. *J Physiol* 499: 255–266, 1997.
22. **Gibbs J, Harrison LM, Stephens JA.** Organization of inputs to motor neurone pools in man. *J Physiol* 485: 245–256, 1995.
23. **Gydikov A, Kosarov D.** Some features of different motor units in human biceps brachii. *Pflügers Arch* 347: 75–88, 1974.
24. **Halliday DM, Rosenberg JR, Breeze P, Conway BA.** Neural spike train synchronization indices: definitions, interpretations, and applications. *IEEE Trans Biomed Eng* 53: 1056–1066, 2006.
25. **Hansen NL, Hansen S, Christensen LO, Petersen NT, Nielsen JB.** Synchronization of lower limb motor unit activity during walking in human subjects. *J Neurophysiol* 86: 1266–1276, 2001.
26. **Harrison LM, Ironton R, Stephens JA.** Cross-correlation analysis of multi-unit EMG recordings in man. *J Neurosci Methods* 40: 171–179, 1991.
27. **Heckman CJ, Binder MD.** Computer simulation of the steady-state input-output function of the cat medial gastrocnemius motor neuron pool. *J Neurophysiol* 65: 952–967, 1991.
28. **Henneman E.** Relation between size of neurons and their susceptibility to discharge. *Science* 126: 1345–1347, 1957.
29. **Hockensmith GB, Lowell SY, Fuglevand AJ.** Common input across motor nuclei mediating precision grip in humans. *J Neurosci* 25: 4560–4564, 2005.
30. **Hoppeler H, Luthi P, Claassen H, Weibel ER, Howald H.** The ultrastructure of the normal human skeletal muscle. A morphometric analysis on untrained men, women and well-trained orienteers. *Pflügers Arch* 344: 217–232, 1973.
31. **Huesler EJ, Maier MA, Hepp-Reymond MC.** EMG activation patterns during force production in precision grip. III. Synchronisation of single motor units. *Exp Brain Res* 134: 441–455, 2000.
32. **Johnson MA, Polgar J, Weightman D, Appleton D.** Data on the distribution of fibre types in thirty-six human muscles. An autopsy study. *J Neurol Sci* 18: 111–129, 1973.
33. **Kanda K, Hashizume K.** Factors causing difference in force output among motor units in the rat medial gastrocnemius muscle. *J Physiol* 448: 677–695, 1992.
34. **Keen DA, Fuglevand AJ.** Common input to motor neurons innervating the same and different compartments of the human extensor digitorum muscle. *J Neurophysiol* 91: 57–62, 2004.
35. **Kernell D.** Organized variability in the neuromuscular system: a survey of task-related adaptations. *Arch Ital Biol* 130: 19–66, 1992.
36. **Kernell D.** Synaptic influence on the repetitive activity elicited in cat lumbosacral motor neurones by long-lasting injected currents. *Acta Physiol Scand* 63: 409–410, 1965.
37. **Kernell D, Eerbeek O, Verhey BA.** Motor unit categorization on basis of contractile properties: an experimental analysis of the composition of the cat's m. peroneus longus. *Exp Brain Res* 50: 211–219, 1983.
38. **Kilner JM, Baker SN, Lemon RN.** A novel algorithm to remove electrical cross-talk between surface EMG recordings and its application to the measurement of short-term synchronisation in humans. *J Physiol* 538: 919–930, 2002.
39. **Kilner JM, Baker SN, Salenius S, Jousmaki V, Hari R, Lemon RN.** Task-dependent modulation of 15–30 Hz coherence between rectified EMGs from human hand and forearm muscles. *J Physiol* 516: 559–570, 1999.
40. **Kleine BU, Stegeman DF, Mund D, Anders C.** Influence of motor neuron firing synchronization on SEMG characteristics in dependence of electrode position. *J Appl Physiol* 91: 1588–1599, 2001.
41. **Lowery MM, Stoykov NS, Kuiken TA.** A simulation study to examine the use of cross-correlation as an estimate of surface EMG cross talk. *J Appl Physiol* 94: 1324–1334, 2003.
42. **Maier MA, Hepp-Reymond MC.** EMG activation patterns during force production in precision grip II Muscular synergies in the spatial and temporal domain. *Exp Brain Res* 103: 123–136, 1995.
43. **McCall GE, Byrnes WC, Dickinson A, Pattany PM, Fleck SJ.** Muscle fiber hypertrophy, hyperplasia, and capillary density in college men after resistance training. *J Appl Physiol* 81: 2004–2012, 1996.
44. **Milner-Brown HS, Stein RB.** The relation between the surface electromyogram and muscular force. *J Physiol* 246: 549–569, 1975.
45. **Milner-Brown HS, Stein RB, Yemm R.** The orderly recruitment of human motor units during voluntary isometric contractions. *J Physiol* 230: 359–370, 1973.
46. **Moritz CT, Barry BK, Pascoe MA, Enoka RM.** Discharge rate variability influences the variation in force fluctuations across the working range of a hand muscle. *J Neurophysiol* 93: 2449–2459, 2005.
47. **Moritz CT, Christou EA, Meyer FG, Enoka RM.** Coherence at 16–32 Hz can be caused by short-term synchrony of motor units. *J Neurophysiol* 94: 105–118, 2005.
48. **Nordstrom MA, Fuglevand AJ, Enoka RM.** Estimating the strength of common input to human motor neurons from the cross-correlogram. *J Physiol* 453: 547–574, 1992.
49. **Person RS, Mishin LN.** Auto- and cross-correlation analysis of the electrical activity of muscles. *Med Electron Biol Eng* 42: 155–159, 1964.
50. **Roeleveld K, Blok JH, Stegeman DF, van Oosterom A.** Volume conduction models for surface EMG; confrontation with measurements. *J Electromyogr Kinesiol* 7: 221–232, 1997.

51. **Rosenfalck P.** Intra- and extracellular potential fields of active nerve and muscle fibers. *Acta Physiol Scand Suppl* 47: 239–246, 1969.
52. **Santello M, Fuglevand AJ.** Role of across-muscle motor unit synchrony for the coordination of forces. *Exp Brain Res* 159: 501–508, 2004.
53. **Sears TA, Stagg D.** Short-term synchronization of intercostal motor neurone activity. *J Physiol* 263: 357–381, 1976.
54. **Semmler JG.** Motor unit synchronization and neuromuscular performance. *Exerc Sport Sci Rev* 30: 8–14, 2002.
55. **Semmler JG, Kornatz KW, Dinenno DV, Zhou S, Enoka RM.** Motor unit synchronisation is enhanced during slow lengthening contractions of a hand muscle. *J Physiol* 545: 681–695, 2002.
56. **Semmler JG, Nordstrom MA.** Motor unit discharge and force tremor in skill- and strength-trained individuals. *Brain Res* 119: 27–38, 1998.
57. **Solomonow M, Baratta R, Zhou B, Lu Y, Zhu M, Acierno S.** Surface and wire EMG crosstalk in neighbouring muscles. *J Electromyogr Kinesiol* 4: 131–142, 1994.
58. **Stålberg E, Antoni L.** Electrophysiological cross section of the motor unit. *J Neurol Neurosurg Psychiatry* 43: 469–474, 1980.
59. **Taylor AM, Steege JW, Enoka RM.** Motor-unit synchronization alters spike-triggered average force in simulated contractions. *J Neurophysiol* 88: 265–276, 2002.
60. **Thomas CK, Ross BH, Stein RB.** Motor-unit recruitment in human first dorsal interosseous muscle for static contractions in three different directions. *J Neurophysiol* 55: 1017–1029, 1986.
61. **Winges SA, Santello M.** Common input to motor units of digit flexors during multi-digit grasping. *J Neurophysiol* 92: 3210–3220, 2004.
62. **Winter DA, Fuglevand AJ, Archer SE.** Crosstalk in surface electromyography: theoretical and practical estimates. *J Electromyogr Kinesiol* 4: 15–26, 1994.
63. **Yao W, Fuglevand AJ, Enoka RM.** Motor-unit synchronization increases EMG amplitude and decreases force steadiness of simulated contractions. *J Neurophysiol* 83: 441–452, 2000.